

# Optimization of the In-Air Cylinders Filling for Emissions Reduction in Diesel Engines

Rabih OMRAN<sup>1</sup>, Rafic YOUNES<sup>2</sup>, Jean-Claude CHAMPOUSSIN<sup>1</sup>

<sup>1</sup> : LMFA - Ecole Centrale de Lyon - France, <sup>2</sup> : Lebanese University Faculty of Engineering - Lebanon

Copyright © 2008 SAE International

## ABSTRACT

Modern diesel engines are typically equipped with common rail injection system, variable geometry turbocharger and exhaust gas recirculation system in order to meet the emissions standards. While the electronic fuel control has been extensively developed and used in the common rail injection systems, the "in-air cylinders filling" control remains poorly exploited. In this paper, we suggest a dynamic engine optimization process that predicts, under transient conditions, the optimal values of the intake pressure and the compressor mass flow rate to be applied to the engine based on pollution criteria such as the opacity. The optimization procedure and a physical mean value model describing the functioning of a variable geometry turbocharged diesel engine and its smoke's opacity are shown in details. The simulations results of the engine's model are in excellent agreement with the experimental data collected on test bench. The optimization results are compared to the engine's simulations using fixed geometry turbocharger, they show enormous gain in opacity reduction which reflects the importance of the air supply system control.

## I. INTRODUCTION

In the last two decades, the turbochargers have more and more gained interest of the engines producers. Their applications reduce the fuel specific consumption; they improve the effective efficiency of the engine and permit its downsizing. Therefore the turbochargers applications have gradually spread to involve direct injection diesel engines of variable size in different sectors: naval propulsion, industrial engines, trains, heavy duty engines, and so on. And recently, in automotive diesel industry, the variable geometry turbocharger has become standard equipment accompanying new engines production.

The use of a turbine with variable geometry provides the required fresh air under different load and engine speed, especially under high load and low crankshaft angular speed where the kinetic energy of the exhaust pressure is not powerful enough to speed up the turbocharger axis and deliver the necessary power to compress the air. At high crankshaft angular speed, the variable geometry of the turbine allows to limit the power transferred from the exhaust gas to the turbine wheels in order to prevent the turbocharger destruction due to thermal or mechanical restrictions [1]. The turbocharger must also have a fast response under transient conditions in order to provide the desired air flow and to reduce the compressor lag time [2]. Actually these criteria have been mostly satisfied but the existing turbochargers are unable to follow the demanding evolution of the future engines and the more restricted pollution legislations fixed in the European emissions standards (table 1); the particulate matter that are mostly emitted under transient conditions due to air insufficiency are expected to be reduced of a ratio 1/10 by 2010 (Euro 6). The nitrogen oxides are also supposed to be reduced to half, its emission is intensified by smaller rate of the recirculated exhaust gas due to insufficiency of the fresh air provided by the compressor. Many researches and ideas are suggested or are actually applied to improve the turbocharger performances such as the bi-turbocharger with waste gate and variable geometry turbine [3], the turbocharger power assist system [2], the electric compressor [4], and so on.

In this paper, we suggest a method to set the technical characteristics of the ideal air management system for which must tend the efforts of the technical research. We propose to use the mean value models to describe the behavior and performance of a heavy duty diesel engine and its smoke's opacity. Then we detailed a dynamic optimization procedure that computes, in transient conditions, the optimal air flow rate and intake pressure required to maximize the engine effective power and to minimize its opacity.

The paper is divided to six sections as follows: I Introduction, II Modeling of turbocharged diesel engine III Validation of the engine's model, IV Optimization over dynamic courses, V Results and Discussion, VI Conclusion and the authors' references.

Heavy duty vehicle	Euro 1 1993	Euro 2 1996	Euro 3 2000	Euro 4 2005	Euro 5 2008	Euro 6 2010
Oxides nitrogen	9	7	5	3,5	2	1
Carbon monoxide	4,5	4	2,1	1,5	1,5	1,5
Hydro-carbons	1,23	1,1	0,66	0,46	0,46	0,46
Particulate Matter	0,4	0,15	0,1	0,02	0,02	0,002

Table 1: European standard of heavy duty vehicles in g/KW.h

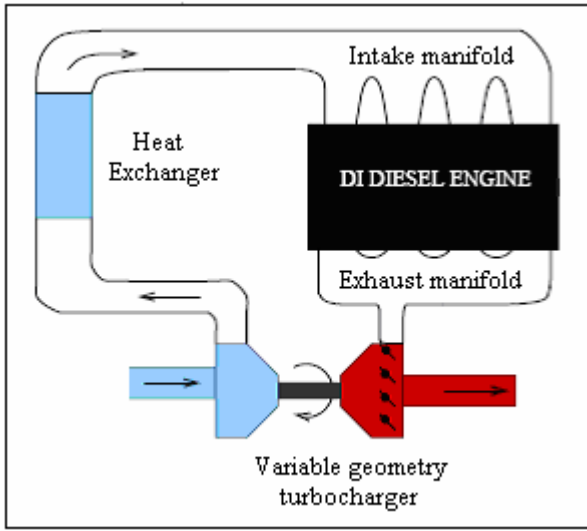


Figure 1: Description of the engine.

## II. MODELING OF TURBOCHARGED DIESEL ENGINE

Diesel engines can be modeled in two different ways: The models of knowledge (quasi-static [5], draining-replenishment [6], semi mixed [7], bond graph), and the models of representation (transfer functions [5], temporal series [8], neural networks [9]).

Seen our optimization objective, the model of knowledge will be adopted in this paper. The mean value model is the simplest analytic approach to be used in an optimization process. The engine described in this paper is a six cylinders heavy duty diesel engine equipped with a variable geometry turbocharger and a water cooled heat exchanger to cool the hot air exiting the compressor (fig. 1). The engine is not equipped with exhaust gas recirculation system that is mainly used to reduce the NO<sub>x</sub> emissions. Consequently the engine can be divided to four main subsystems: the intake manifold, the engine, the exhaust manifold and the turbocharger. Each subsystem will be modeled separately.

### II.1. Intake manifold

The air is considered as an ideal gas and is described by the ideal gas state equation:

$$p_a \cdot V_a = m_a \cdot R \cdot T_a \quad (1)$$

$p_a$ ,  $V_a$  and  $T_a$  are the pressure, the volume and the temperature of the air in the intake manifold respectively and  $R$  is the mass constant of the air. Considering that the air temperature in the intake manifold varies slowly, we will neglect the intake temperature variation against the air mass variation in order to simplify the problem. Therefore differentiating (1) and neglecting the temperature variation gives [7]:

$$\dot{p}_a = \frac{\dot{m}_a \cdot R \cdot T_a}{V_a} \quad (2)$$

The heat losses are also neglected through the manifold walls and the intake manifold is considered as an open system. Applying the principle of the energy conservation to the intake manifold gives:

$$C_v \cdot \frac{d(m_a \cdot T_a)}{dt} = C_p \cdot (\dot{m}_c \cdot T_{HE} - \dot{m}_{ai} \cdot T_a) \quad (3)$$

$C_v$  and  $C_p$  are the heat capacities at constant volume and pressure,  $\dot{m}_c$  is the compressor air mass flow rate,  $\dot{m}_{ai}$  is the air mass flow rate entering the engine and  $T_{HE}$  is the temperature of the air exiting the cooling water heat exchanger. Neglecting the intake temperature variation against the air mass variation, equation (3) gives:

$$\dot{m}_a \cdot T_a = \gamma_a \cdot (\dot{m}_c \cdot T_{HE} - \dot{m}_{ai} \cdot T_a) \quad (4)$$

$\gamma_a$  is the ratio of the heat capacities at constant pressure and volume.

The air mass change in the intake manifold is computed using the mass conservation principle:

$$\dot{m}_a = \dot{m}_c - \dot{m}_{ai} \quad (5)$$

By replacing (5) in (4), the intake temperature is deduced using the following equation:

$$T_a = \frac{\gamma_a \cdot \dot{m}_c}{\dot{m}_c + (\gamma_a - 1) \cdot \dot{m}_{ai}} \cdot T_{HE} \quad (6)$$

The air mass flow rate  $\dot{m}_{ai}$  entering the engine is given by :

$$\dot{m}_{ai} = \eta_v \cdot \dot{m}_{ai,th} \quad (7)$$

$\eta_v$  is the volumetric efficiency and  $\dot{m}_{ai,th}$  is the theoretical air mass flow rate capable of filling the cylinders volume at the intake pressure and temperature conditions:

$$\dot{m}_{ai,th} = \frac{N_{cyl} \cdot V_{cyl} \cdot \omega \cdot p_a}{4 \cdot \pi \cdot R \cdot T_a} \quad (8)$$

$N_{cyl}$  is the total number of cylinders,  $V_{cyl}$  is the displacement of one cylinder,  $\omega$  is the engine angular

speed. The volumetric efficiency is computed using the semi-empirical equation:

$$\eta_v = \alpha_0 + \alpha_1 \omega + \alpha_2 \omega^2 \quad (9)$$

where  $\alpha_i$  are constants identified from experimental data using the least square method. The hot air exiting the compressor is cooled by a water cooled heat exchanger before entering the intake manifold, the temperature  $T_{HE}$  is computed using the following equation:

$$T_{HE} = (1 - \eta_{HE}) \cdot T_c + \eta_{HE} \cdot T_{water} \quad (10)$$

$T_c$  is the temperature of the air at the compressor's exit,  $T_{water}$  is the temperature of the cooling water supposed constant and  $\eta_{HE}$  is the efficiency of the heat exchanger also supposed constant. The temperature  $T_c$  can be computed using the isentropic efficiency of the compressor:

$$T_c = T_0 \left( 1 + \left( \left( \frac{p_a}{p_0} \right)^{\frac{\gamma_a - 1}{\gamma_a}} - 1 \right) \frac{1}{\eta_c} \right) \quad (11)$$

$p_0$  and  $T_0$  are the atmospheric pressure and temperature and  $\eta_c$  is the isentropic efficiency of the compressor.

## II.2. Engine

The fundamental principle of the dynamic applied to the crankshaft gives:

$$\frac{d}{dt} \left( \frac{I}{2} J(\theta) \omega^2 \right) = P_e - P_r \quad (12)$$

$J(\theta)$  is the moment of inertia of the engine, it is a periodic function of the crankshaft angular position due to the repeated motion of its pistons and connecting rods. For simplicity, in this paper, the inertia is considered constant.  $P_e$  is the effective power produced by the engine:

$$P_e = \eta_e \cdot \dot{m}_f \cdot H_f \quad (13)$$

$\dot{m}_f$  is the fuel mass flow rate,  $H_f$  is the fuel heating value and  $\eta_e$  is the effective efficiency of the engine given by:

$$\eta_e = \lambda \cdot \left( \frac{c_1 + c_2 \cdot \lambda + c_3 \cdot \lambda^2 + c_4 \cdot \lambda \cdot \omega}{c_5 \cdot \lambda^2 \cdot \omega + c_6 \cdot \lambda \cdot \omega^2 + c_7 \cdot \lambda^2 \cdot \omega^2} \right) \quad (14)$$

$c_i$  are constants, and  $\lambda$  is the air to fuel ratio:

$$\lambda = \frac{\dot{m}_{ai}}{\dot{m}_f} \quad (15)$$

$P_r$  is the friction power.  $C_r$  is the engine's load, it is the friction torque applied to the engine's crankshaft and controlled via a brake dynamometer:

$$P_r = C_r \omega \quad (16)$$

Figure 2 represents a comparison between the effective efficiency computed using (14) and the experimental data measured over a test bench. The model outputs show good agreement when compared to the experimental data.

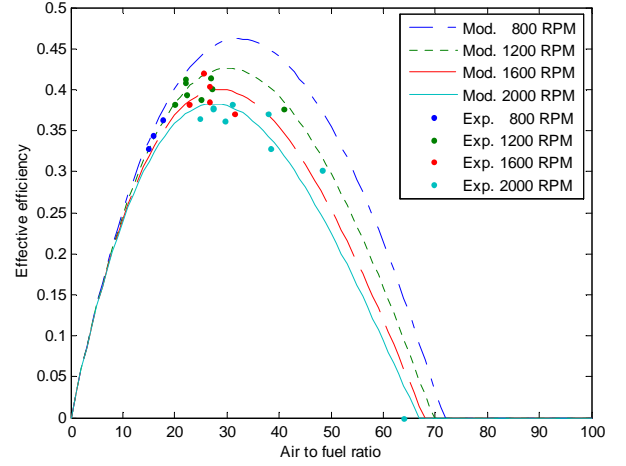


Figure 2: Comparison between the model's outputs of the effective efficiency computed using (14) and the experimental data for different crankshaft angular speed.

## II.3. Exhaust manifold

Neglecting the heat losses through the manifold walls and considering the exhaust gas as an ideal gas with constant specific heats, the differential equation of the exhaust pressure is computed using the principle of the energy conservation and the ideal gas state equation [8]:

$$\dot{p}_e = \frac{\gamma_e \cdot R \cdot (\dot{m}_t \cdot T_e - \dot{m}_{eo} \cdot T_{eo})}{V_e} \quad (17)$$

$p_e$ ,  $V_e$  and  $T_e$  are the pressure, the volume and the temperature of the air in the exhaust manifold respectively,  $\gamma_e$  is the ratio of the heat capacities at constant volume and pressure,  $\dot{m}_t$  is the turbine mass flow rate,  $\dot{m}_{eo}$  and  $T_{eo}$  are the gas mass flow rate and temperature exiting the engine respectively.  $\dot{m}_{eo}$  is computed using the following equation:

$$\dot{m}_{eo} = \dot{m}_f + \dot{m}_{ai} \quad (18)$$

$T_{eo}$  is expressed by the following semi-empirical equation:

$$T_{eo} = T_a + \frac{b_1 + b_2 \cdot \lambda + b_3 \cdot \lambda^2}{1.2 + \frac{\lambda}{15}} + \frac{b_4}{\omega} + b_5 \quad (19)$$

$\dot{m}_f$  is the fuel mass flow rate and  $b_i$  are constants identified from experimental data. Figure 3 shows that the model's outputs using (19) are in good agreement with the experimental data.

The gas mass change in the exhaust manifold is computed using the mass conservation principle:

$$\dot{m}_e = \dot{m}_{ai} + \dot{m}_f - \dot{m}_t \quad (20)$$

The temperature of the gas in the exhaust manifold is deduced from the ideal gas state equation:

$$T_e = \frac{p_e \cdot V_e}{m_e \cdot R} \quad (21)$$

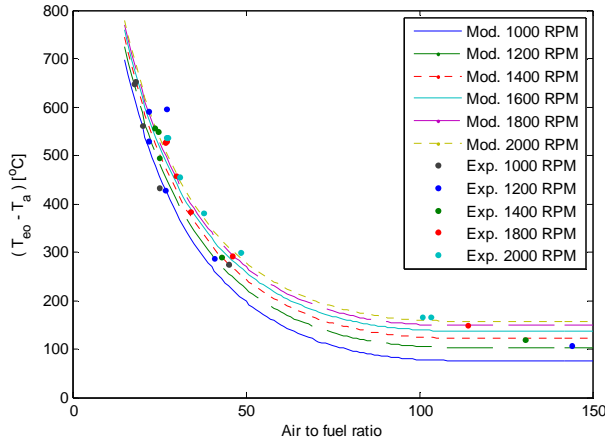


Figure 3: Comparison between the temperature difference values of the gas exiting the engine and the intake manifold computed using (19) and the experimental data for different crankshaft angular speed.

#### II.4. Turbocharger model

The turbocharger modeling process [10] can be divided into three parts: the compressor, the turbine and the mechanical coupling. Each part will be described separately.

##### II.4.a. Compressor model

The air mass flow rate exiting the compressor is expressed by the following semi-empirical equation:

$$\dot{m}_c = \Phi \cdot \frac{P_0}{RT_0} \cdot \frac{\pi}{4} D_c^2 U_c \quad (22)$$

$D_c$  is the diameter of the compressor wheel,  $U_c$  is the air velocity at the extremity of the compressor blades, it is proportional to the angular speed of the compressor shaft and is expressed by:

$$U_c = \frac{\pi}{60} \cdot D_c \cdot N_{tc} \quad (23)$$

$\Phi$  is expressed by:

$$\Phi = \frac{k_3 \Psi - k_1}{k_2 + \Psi} \quad (24)$$

$$k_i = k_{i1} + k_{i2} \cdot M \quad (25)$$

$k_{ij}$  are constants,  $M$  is the Mach number, it is the ratio of the blade velocity  $U_c$  to the velocity of sound:

$$M = \frac{U_c}{\sqrt{\gamma \cdot R \cdot T_0}} \quad (26)$$

$\Psi$  is given by the following equation:

$$\Psi = \frac{C_p T_0 \left( (\pi_c)^{\frac{\gamma-1}{\gamma}} - 1 \right)}{0.5 U_c^2} \quad (27)$$

$C_p$  is the heat capacity of air at constant pressure and  $\pi_c$  is the compression ratio of the compressor:

$$\pi_c = \frac{p_a}{p_0} \quad (28)$$

The power consumed by the compressor is expressed by:

$$P_c = \dot{m}_c C_p T_0 \left( (\pi_c)^{\frac{\gamma-1}{\gamma}} - 1 \right) \frac{1}{\eta_c} \quad (29)$$

$\eta_c$  is the isentropic efficiency, expressed by :

$$\eta_c = c_0 + c_1 \Phi + c_2 \Phi^2 \quad (30)$$

$c_i$  are variables given by :

$$c_i = d_{i1} + d_{i2} \cdot M + d_{i3} \cdot M^2 \quad (31)$$

$d_{ij}$  are constants identified from the compressor experimental maps provided by the turbocharger producer.

Figures 4 and 5 represent the graphs of the compressor mass flow rate and the isentropic efficiency computed using (22) and (30) respectively; the models' results are in good agreement with the producer experimental data.

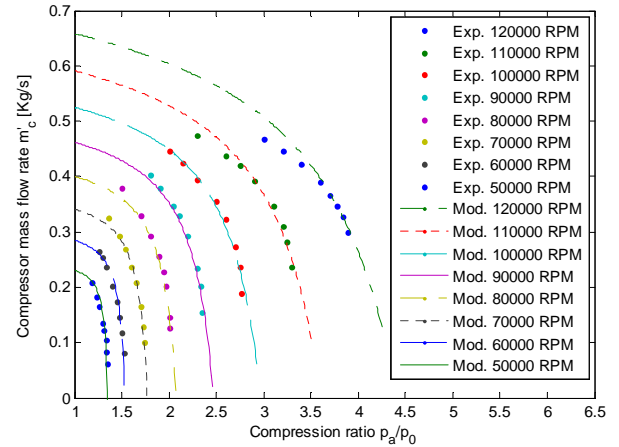


Figure 4: Comparison between the values of the compressor mass flow rate computed using (22) and the experimental data for different turbocharger angular speed.

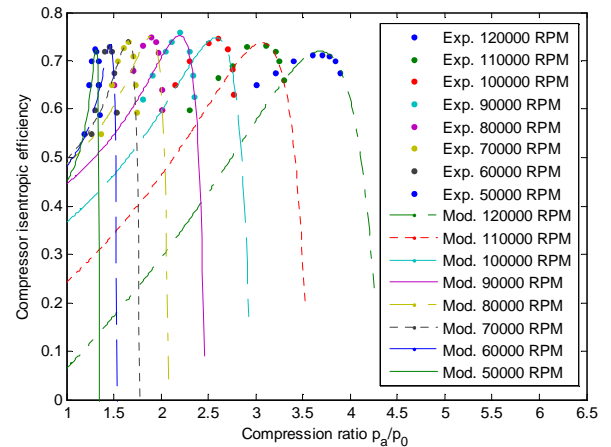


Figure 5: Comparison between the values of the compressor isentropic efficiency computed using (30) and the experimental data for different turbocharger angular speed.

##### II.4.b. Turbine Model

The turbine mass flow rate  $\dot{m}_t$  is expressed by the following equation:

$$\left\{ \frac{\dot{m}_t \cdot \sqrt{T_e}}{p_e \cdot 10^{-3}} = \frac{\sqrt{T_{ref}}}{p_{ref}} \cdot [2 \cdot \pi_t \cdot (1 - \pi_t)]^{0.5} \dots \right. \quad (32)$$

$$\left. \dots (h_1 \cdot GV + h_2) \cdot \left[ h_3 \cdot \left( \frac{1}{\pi_t} - 1 \right) + h_4 \right] \right\}$$

$\left\{ \frac{\dot{m}_t \cdot \sqrt{T_e}}{p_e \cdot 10^{-3}} \right\}$  is the corrected mass flow rate of the turbine.

$p_{ref}$  and  $T_{ref}$  are the pressure and temperature of reference given by the turbocharger producer, they describe the air state conditions used when the turbocharger charts were drawn,  $\gamma_e$  is the ratio of the heat capacities at constant pressure and volume, at the temperature  $T_e$  and  $\pi_t$  is the turbine relaxation ratio:

$$\pi_t = \frac{p_0}{p_e} \quad (33)$$

GV is a real number varying between 0 and 1. It describes the change in the palettes opening position of a turbine with variable geometry which varies the air effective cross section of the turbine. In the case of a fixed geometry turbocharger, GV is set to zero.

The power produced by the turbine is expressed by:

$$P_t = \dot{m}_t \cdot C_{pe} \cdot T_e \cdot \left( 1 - (\pi_t)^{\frac{\gamma_e - 1}{\gamma_e}} \right) \cdot \eta_t \quad (34)$$

$\eta_t$  is the isentropic efficiency of the turbine expressed by:

$$\eta_t = k_1 + k_2 \left( \frac{U}{C} \right) + k_3 \left( \frac{U}{C} \right)^2 + k_4 \left( \frac{U}{C} \right)^3 \quad (35)$$

$k_i$  are variables expressed by:

$$k_i = \begin{pmatrix} k_{i1} + k_{i2} \cdot N_{tc} + k_{i3} \cdot N_{tc}^2 + k_{i4} \cdot GV \\ + k_{i5} \cdot GV^2 + k_{i6} \cdot N_{tc} \cdot GV \end{pmatrix} \quad (36)$$

$k_{ij}$  are constants identified from the turbocharger experimental data.

$$\frac{U}{C} = \frac{\pi N_{tc} D_t}{60 \sqrt{2 C_{pe} T_e \left( 1 - (\pi_t)^{\frac{\gamma_e - 1}{\gamma_e}} \right)}} \quad (37)$$

$D_t$  is the diameter of the turbine's wheels and  $C_{pe}$  is the heat capacity of air at constant pressure, at the temperature  $T_e$ .

Figures 6-8 show a comparison between the turbine mass flow rate and the isentropic efficiency values computed using (32) and (35) respectively and the experimental data for different positions of the variable geometry GV. The models results are in good agreement with the experimental data provided by the producer.

#### II.4.c. The mechanical coupling

The fundamental principle of the dynamic applied to the rotating shaft of the turbocharger gives:

$$\frac{d}{dt} \left( \frac{1}{2} I_{tc} \omega_{tc}^2 \right) = \eta_m \cdot P_t - P_c \quad (38)$$

$I_{tc}$  and  $\eta_m$  are the moment of inertia and the mechanical efficiency of the turbocharger.

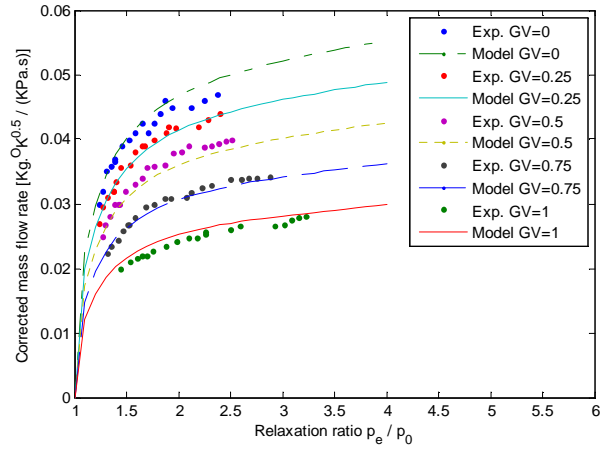


Figure 6: comparison between the model's outputs of the corrected turbine mass flow rate of the turbine ( $\dot{m}_t \cdot T_e^{0.5} / p_e \cdot 10^{-3}$ ) computed using (32) and the experimental data for different GV positions.

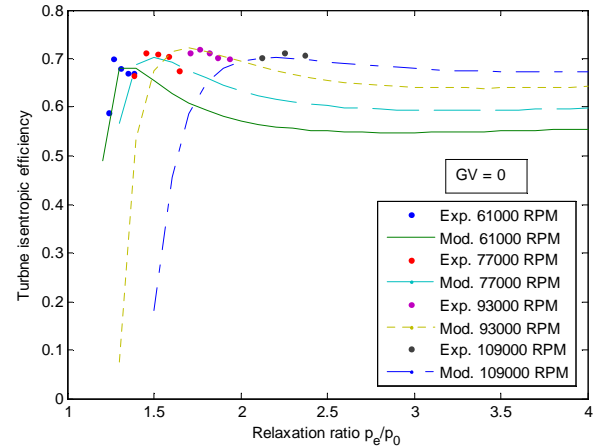


Figure 7: Comparison between the model's outputs of the turbine isentropic efficiency computed using (35) and the experimental for different turbocharger angular speed and at a constant opening of the geometry variable ( $GV = 0$ ).

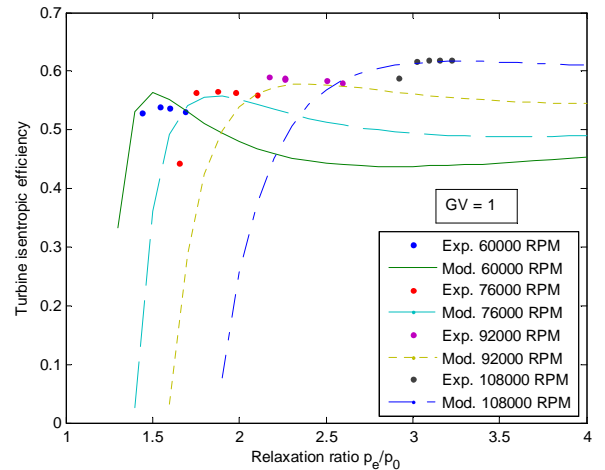


Figure 8: Comparison between the model's outputs of the turbine isentropic efficiency computed using (35) and the experimental for different turbocharger angular speed and at a constant opening of the geometry variable ( $GV = 1$ ).

## II.5. Opacity model

The pollutants that characterize the diesel engines are mainly the oxides of nitrogen and the particulate matter. In our work, the PM is described by the opacity which is computed using the following equation [5] (fig. 9):

$$Op = c_1 \cdot \omega^{c_2} \cdot \dot{m}_{ai}^{c_3 \cdot \omega + c_4} \cdot \dot{m}_f^{c_5 \cdot \omega + c_6} \quad (39)$$

$c_i$  are constants identified from the experimental data measured over a test bench.

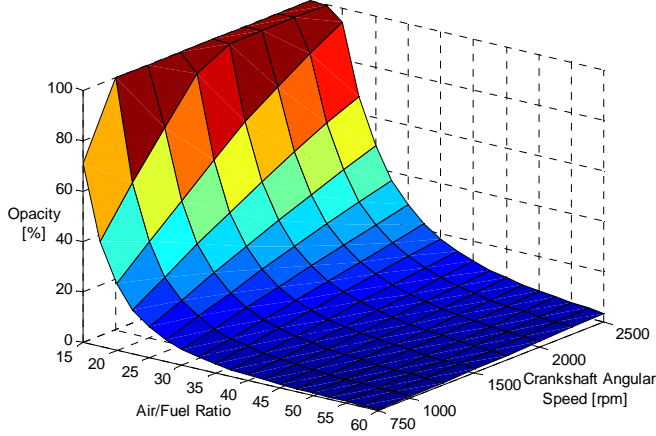


Figure 9: Graphical representation of the opacity model outputs computed using (39) at constant fuel flow rate 6 g/s.

## II.6. Engine complete model

Reassembling the different subsystems' equations leads to the complete engine model describing the functioning and performance of a variable geometry turbocharged diesel engine. The model is characterized by five state variables  $p_a, p_e, m_e, \omega, \omega_{ic}$ , two input variables  $\dot{m}_f$  and  $C_r$ , one control variable  $GV$  and the following five differential equations representing the different dynamic processes in the system:

$$\begin{cases} (2) \rightarrow \dot{p}_a = \frac{\dot{m}_a \cdot R \cdot T_a}{V_a} \\ (17) \rightarrow \dot{p}_e = \frac{\gamma_e \cdot R \cdot (\dot{m}_i \cdot T_e - \dot{m}_{eo} \cdot T_{eo})}{V_e} \\ (20) \rightarrow \dot{m}_e = \dot{m}_{ai} + \dot{m}_f - \dot{m}_i \\ (38) \rightarrow \frac{d}{dt} \left( \frac{1}{2} I_{ic} \omega_{ic}^2 \right) = \eta_m \cdot P_t - P_c \\ (12) \rightarrow \frac{d}{dt} \left( \frac{1}{2} J \omega^2 \right) = \eta_e \cdot \dot{m}_f \cdot H_f - C_r \cdot \omega \end{cases} \quad (40)$$

## III. VALIDATION OF THE ENGINE'S MODEL

The test bench used for the experimental study involves a 6 cylinders turbocharged diesel engine, an Eddy current brake, a Bosch smoke detector and various

sensors to measure the gas state variables in the different engine's subsystems. Engine's characteristics are reported in table 2.

Stroke [mm]	145
Displacement [l]	9,84
Compression ratio	17/1
Bore [mm]	120
Maximum Power [KW]	260
at crankshaft angular speed [rpm]	2400
Maximum torque [N.m]	1580
at crankshaft angular speed [rpm]	1200
Boost pressure [bar]	3

Table 2: Engine Characteristics

Figures 10 and 11 show a comparison between two simulations results of the engine complete model (ref. section II.6) and the experimental data. The figures include the input and control variables profiles ( $\dot{m}_f, C_r$  and  $GV$ ) and the evolution of the opacity and the following state variables  $\omega, \omega_{ic}, p_a, p_e$ . The differential equations described in section II.6 are computed simultaneously using the Runge-Kutta method. We note that these simulations are characterized by simultaneous changes in the input and control variables. The simulations results are in good agreement with the experimental data.

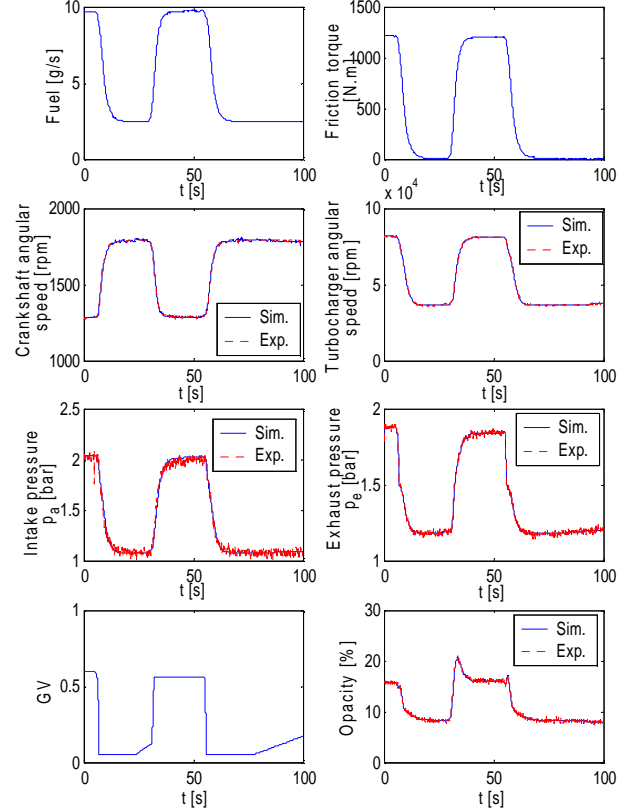


Figure 10: Validation of the complete engine model under dynamic load (example 1).

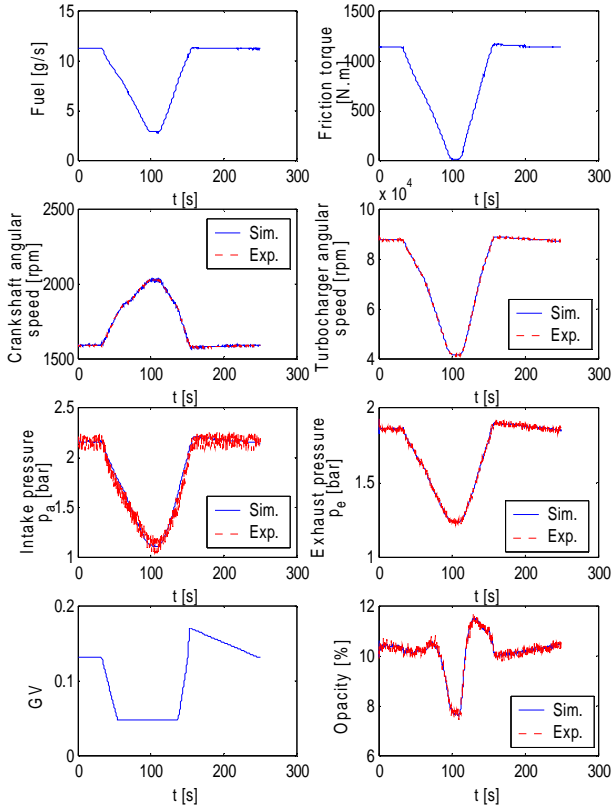


Figure 11: Validation of the complete engine model under dynamic load (example 2).

## IV. OPTIMIZATION OVER DYNAMIC COURSES

### IV.1. Description of the problem

When conceiving an engine, engines producers have always to confront and solve the contradictory tasks of producing maximum power (or minimum fuel consumption) while respecting several pollution constraints (European norms). In vehicles, the emissions reduction is classically done in two steps: at the source by using different equipments (variable geometry turbocharger, exhaust gas recirculation system, common rail injection system, ...) and control schemes (Electronic Control Unit ECU), and at the exhaust of the gases, by using different systems of post-treatment (Diesel Oxidation Catalyst, Selective Catalytic Reduction SCR, NOx traps ...).

In this paper, we focused on resolving the pollution problem at the source, by searching for the optimal "in-air cylinders filling" to be applied to the engine. Consequently, the problem can now be defined; it consists in the following multi-criteria objective:

$$\begin{cases} \text{Maximize "Power"} \\ \text{Minimize "Emissions"} \end{cases} \quad (41)$$

This complex two-dimensional objective can be replaced by a single mathematical function regrouping the two previous criteria:

$$f = -\int \frac{P}{P_{\max}} \cdot dt + \sum_i \left\{ \int \frac{E_i}{E_{i,\max}} \cdot dt \right\} \quad (42)$$

$P$  is the engine effective power,  $E_i$  is the different emissions, and the indication  $\max$  characterizes the maximum value that a variable can reach. The integral represents the heap of the pollutants and power over a given dynamic course. This course can be, as an example, a part of the European Transient Cycle (ETC). We chose this form of the objective function because the engine usually runs under dynamic load. Consequently an efficient optimization process must take into consideration the dynamic response of the engine. In this paper we will only use the opacity (eq. 39) as a pollution criterion seen the simplicity of the model and the priority given to the presentation of the method, but we should note that the optimization process is universal and it can involve as many emissions' criteria as we want. The function "objective" becomes:

$$f = -\int \frac{P}{P_{\max}} \cdot dt + \int \frac{Op}{Op_{\max}} \cdot dt \quad (43)$$

### IV.2. Formulation of the problem

The problem consists therefore in minimizing the following function "objective" computed using (13) and (39) over a definite working interval  $[0, t]$ :

$$f = \left\{ \begin{array}{l} -\frac{H_f}{P_{\max}} \cdot \int \eta_e \cdot \dot{m}_f \cdot dt \\ + \frac{c_1}{Op_{\max}} \cdot \int \omega^{c_2} \cdot \dot{m}_{ai}^{c_3 \cdot \omega + c_4} \cdot \dot{m}_f^{c_5 \cdot \omega + c_6} \cdot dt \end{array} \right\} \quad (44)$$

under the equalities constraints representing the differential equations of the engine (eq. 12) and the intake manifold (eq. 2) :

$$\begin{cases} (2) \rightarrow \dot{p}_a = \frac{r \cdot T_a \cdot (\dot{m}_c - \dot{m}_{ai})}{V_a} \\ (12) \rightarrow \frac{d}{dt} \left( \frac{1}{2} J \omega^2 \right) = \eta_e \cdot \dot{m}_f \cdot H_f - C_r \cdot \omega \end{cases} \quad (45)$$

and the inequalities constraints derived from the physical and mechanical restrictions of the air to fuel ratio, the intake pressure and the crankshaft angular speed:

$$\begin{cases} 15 \leq \lambda \leq 100 \\ 9.5 \cdot 10^4 \leq p_a \leq 30 \cdot 10^4 \text{ [Pa]} \\ 83 \leq \omega \leq 260 \text{ [rd/s]} \end{cases} \quad (46)$$

$\lambda$  is computed using (7), (8) and (15):

$$\lambda = \frac{(\alpha_0 + \alpha_1 \omega + \alpha_2 \omega^2) \cdot N_{cyl} \cdot V_{cyl} \cdot \omega \cdot p_a}{4 \cdot \pi \cdot \dot{m}_f} \quad (47)$$

The input variables of the optimization problem are  $C_r(t)$  and  $\dot{m}_f(t)$ , and the output variables are  $\omega(t)$ ,  $p_a(t)$  and  $\dot{m}_c(t)$ .

We intentionally eliminate the exhaust manifold and turbocharger differential equations from the equalities constraints because our objective is to find the optimal "in-air cylinders filling"  $p_a(t)$  and  $\dot{m}_c(t)$  without being limited to any engine equipments such as the variable geometry turbocharger early described. In other words,

we can consider that we added to the existing turbocharger a power assist device or that we replaced it by a special instrument that can deliver to the intake manifold any desired value of the air mass flow rate at any time. We formulated the optimization problem in this form in order to deduce the characteristics of the optimal air supply system that the engine must be equipped with. Afterward these characteristics will be used to properly choose the correct size, type and power of the optimal air supply device. Later, in the conclusion, we present several devices that can be used to provide these optimal values.

### IV.3. Problem Discretization

There is no analytic solution to the problem previously formulated; therefore there is a necessity to reformulate it in its discretized form. The integrals in the function "objective" (eq. 44) become a simple sum of the functions computed at different instant  $t_i$ :

$$(44) \rightarrow f = \left\{ \begin{array}{l} -\frac{H_f}{P_{\max}} \cdot \sum_{i=1}^N [\eta_e \cdot \dot{m}_f]_{(i)} \\ + \frac{c_1}{Op_{\max}} \cdot \sum_{i=1}^N [\omega^{c_2} \cdot \dot{m}_{ai}^{c_3 \cdot w + c_4} \cdot \dot{m}_f^{c_5 \cdot w + c_6}]_{(i)} \end{array} \right\} \quad (48)$$

$N$  is the number of the discretized points. The optimization variables are  $\omega_{(i)}$ ,  $p_{a(i)}$  and  $\dot{m}_{c(i)}$  at different instant  $t_i$ , so in total the problem has  $3 \times N$  optimization variables. Using the Taylor development truncated at the first differential order, the equalities constraints (eq. 45) give:

$$\left\{ \begin{array}{l} p_{a(i+1)} - p_{a(i)} - \frac{h}{V_a} (r \cdot T_a \cdot (\dot{m}_{c(i)} - \dot{m}_{ai(i)})) = 0 \\ \omega^2_{(i+1)} - \omega^2_{(i)} - \frac{2 \cdot h}{J} (\eta_e \cdot \dot{m}_f \cdot H_f - C_{r(i)} \cdot \omega_{(i)}) = 0 \end{array} \right. \quad (49)$$

$h$  is the time step. For  $N$  discretized points, we have  $2 \times (N-1)$  equalities constraints. The inequalities constraints (eq. 46) in discretized form give:

$$\left\{ \begin{array}{l} 15 \leq \lambda_{(i)} \leq 100 \\ 9.5 \cdot 10^4 \leq p_{a(i)} \leq 30 \cdot 10^4 \quad [Pa] \\ 83 \leq \omega_{(i)} \leq 260 \quad [rd/s] \end{array} \right. \quad (50)$$

For  $N$  discretized points, we have  $6 \times N$  inequalities constraints.

### IV.4. Solution of the optimization problem

The optimization problem under equality and inequality constraints can be described by the following mathematical form:

$$\left\{ \begin{array}{l} \text{Min}\{f(X)\} \\ X = (\omega_{(1)}, \dots, \omega_{(N)}, p_{a(1)}, \dots, p_{a(N)}, \dot{m}_{c(1)}, \dots, \dot{m}_{c(N)}) \\ \text{Under Constraints} \\ h_i(X) = 0 \quad i = 1, \dots, m \\ g_j(X) \leq 0 \quad j = 1, \dots, p \end{array} \right. \quad (51)$$

$f(X)$ ,  $g(X)$  and  $h(X)$  are the objective function, the equalities constraints and the inequalities constraints respectively that are described in (48)-(50). The easiest way of solving such a difficult problem is to reduce it to a problem without constraints by creating a global objective function which regroups: the original function "objective", the equalities constraints with Lagrange multipliers, and the inequalities constraints with a penalty factor [11]. The final objective function becomes:

$$L(X, \lambda) = f(X) + \sum_{i=1}^m \lambda_i \cdot h_i(X) + r \cdot \sum_{j=1}^p [g_j(X)]^2 \quad (52)$$

The problem has  $m$  additional unknown variables (Lagrange's multipliers  $\lambda_i$ ) to be determined in addition to the optimization variables. The optimization algorithm used in this paper is the Broyden-Fletcher-Goldfarb-Shanno B.F.G.S. algorithm.

## V. RESULTS AND DISCUSSION

In this section we present the application results of the optimization procedure over two examples characterized by two different profiles of input variables (fuel mass flow rate and friction torque). The step of discretization  $h$  and the time interval are equal to 0.01s and 3s respectively, so the optimization problem involves (section IV.3):  $N=300$  discretized points, 900 ( $3 \times N$ ) output variables ( $\omega, p_a, \dot{m}_c$ ) with 598 ( $2 \times (N-1)$ ) equalities constraints and 1800 ( $6 \times N$ ) inequalities constraints. Figures 12 and 13 show a comparison between the compressor flow rate and intake pressure given by the optimization process and the ones computed using the engine's complete model (section II.6) for a fixed geometry turbocharger ( $GV = 0$ ). We used the complete engine model with a fixed geometry turbocharger ( $GV = 0$ ) as a comparison tool to show the efficiency of the optimization process and the importance of the "in-air cylinders filling" control.

The optimization results show that we need significantly higher compressor flow rate and intake pressure to reduce the opacity and maximize the effective power.

Figures 14 and 15 show a comparison between the simulated opacity derived from the optimization process and the engine complete model results. The enormous gain in opacity reduction clearly shows the importance of the suggested optimization procedure.

This optimization technique can be exploited to set the characteristics of the optimal air supply device that must be used to maximize the engine performance and minimize its emissions. These characteristics can be defined for example by searching for the optimal "in-air

cylinders filling” over different courses that include severe accelerations, under high load and starting at low crankshaft angular speed. Then these results are compared to the characteristics of the existing commercial turbochargers or more sophisticated air supply devices and finally the most suitable one can be chosen. The chosen turbocharger can also be modeled using the method described in section II.4 and the simulations results of the engine model equipped with the new turbocharger can then be compared to the optimization results obtained in section IV. This technique can also be used to set the characteristics of the air supply device that the automotive engineers and producers much provide in order to improve the performance of the diesel engines.

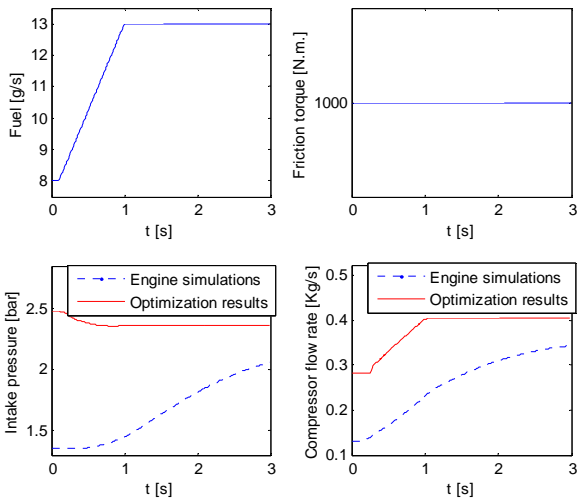


Figure 12: Comparison between the compressor flow rate and the intake pressure given by the optimization procedure and the ones computed using the engine complete model for a variable fuel flow rate and a constant friction torque (1000 N.m).

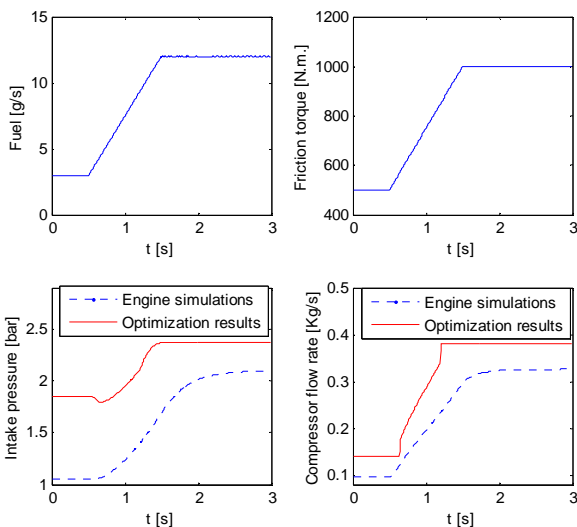


Figure 13: Comparison between the compressor flow rate and the intake pressure given by the optimization procedure and the ones computed using the engine's complete model for a variable fuel flow rate and a variable friction torque.

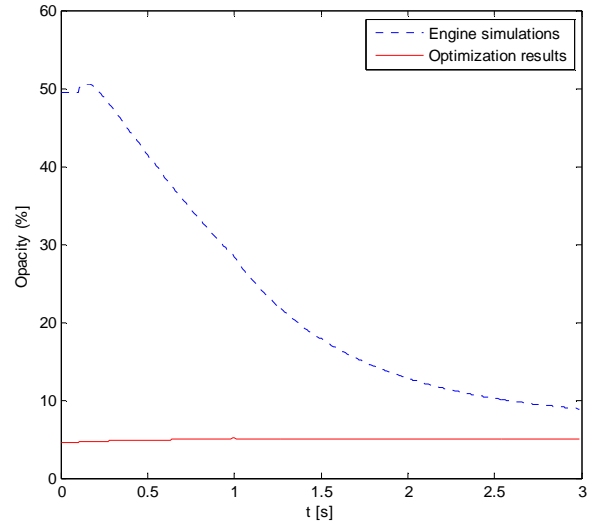


Figure 14: Opacity reduction using the optimal values of the compressor flow rate and intake pressure. The engine is at the same conditions described in fig. 12.

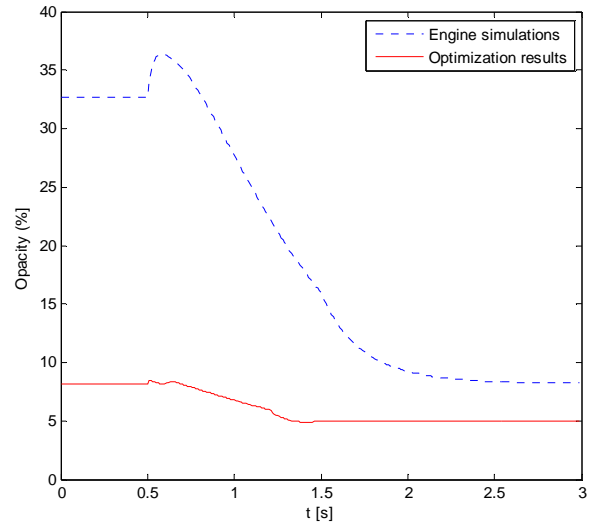


Figure 15: Opacity reduction using the optimal values of the compressor mass flow rate and intake pressure. The engine is at the same conditions described in fig. 13.

## VI. CONCLUSION

We successfully developed and validated a mean value physical model that describes the functioning, the state variables evolution and the opacity of a diesel engine with a variable geometry turbocharger. The simulation results are in good agreement with the dynamic experimental data measured on dynamic test bench (fig. 10-11).

Then we proposed a dynamic optimization procedure that search for the optimal “in-air cylinders filling” in order to minimize the opacity while enhancing the engine performance. The optimization process is described in detail in section IV. The optimization results (fig. 12-13) and the enormous gain in opacity reduction (fig. 14-15) show the importance of the air supply system control. In

addition, the optimization technique using the opacity criterion can be applied to other emissions which have available model.

The suggested optimization procedure can also be used to determine the optimal size, type and power of the air supply device in order to obtain the optimal engine performance at different crankshaft angular speed and load.

Finally, while we did find, in theory, the optimal compressor mass flow rate and intake pressure necessary to minimize the opacity and maximize the effective power, we didn't discuss in details the mechanical equipments required to provide the optimal "in-air cylinders filling". The use of a turbocharger with variable geometry and/or with Waste-Gate and/or power assist system and/or electric compressor is to be considered. In addition, the practical implementation of the dynamic air control is an important task to be studied thereafter.

## REFERENCES

- [1] Z. Filipi, Y. Wang, D. Assanis, "Effect of variable geometry (VGT) on Diesel engine and vehicle system transient response", SAE paper 2001-01-1247, 2001.
- [2] A. Stefanopolou, I. Kolmanovsky, "Evaluation of turbocharger power assist system using optimal control techniques", SAE paper 2000-01-0519, 2000.
- [3] S. Saulnier, S. Soltani, "Computational Study of Diesel Engine Downsizing Using Two-Stage Turbocharging", SAE paper 2004-01-0929, 2004.
- [4] J. Dixon, S.C. George, "Optimal Boost Control for An Electrical Supercharging Application", SAE paper 2004-01-0523, 2004.
- [5] R. Younes, "Elaboration d'un modèle de connaissance du moteur diesel avec turbocompresseur à géométrie variable en vue de l'optimisation de ses émissions", PHD Thesis, Ecole Centrale de Lyon, France, 1993.
- [6] M. Kao, J.J. Moskwa, "Turbocharged Diesel Engine Modeling for Nonlinear Engine Control and State Estimation", ASME Journal of Dynamic Systems, Measurement, and Control, 117: 20-30, March 1995.
- [7] X. Dovifaaz, "Modélisation et commande de moteur Diesel en vue de la réduction de ses émissions", PHD Thesis, UPJV, Amiens, France, 2001.
- [8] S. Ouenou-Gamo, "Modélisation d'un moteur Diesel suralimenté", PHD Thesis, UPJV, Amiens, France, 2001.
- [9] M. Ouladsine, G. Bloch, X. Dovifaaz, "Neural Modelling and Control of a Diesel Engine with Pollution Constraints", Journal of Intelligent and Robotic Systems; Theory and Application, 2004.
- [10] P. Moorai, I. Kolmanovsky, "Turbocharger modeling for automotive control applications", SAE paper, 1999-01-0908, 1999.
- [11] M. Minoux, "Programmation mathématique : Théorie et Algorithmes", Edition Dunod, France, 1983.

## ACRONYMS & ABBREVIATIONS

SYMBOLS	
$\omega$	Crankshaft angular speed [rd/s]
$GV$	Opening position of the turbine's variable geometry
EGR	Exhaust gas recirculation
VGT	Variable geometry turbocharger
$p$	Pressure [Pa]
$V$	Volume [ $m^3$ ]
$T$	Temperature [ $^{\circ}K$ ]
$m'$	mass flow rate [Kg/s]
$N_{tc}$	Turbocharger angular speed [rpm]
$\omega_{tc}$	Turbocharger angular speed [rd/s]
$N_{cyl}$	Cylinder's number
$V_{cyl}$	Displacement [ $m^3$ ]
$\eta_v$	Volumetric efficiency
$\eta_e$	Effective efficiency of the engine
$\eta_{HE}$	Heat exchanger efficiency
$\eta_c$	Compressor isentropic efficiency
$\eta_t$	Turbine isentropic efficiency
$\eta_m$	Turbocharger mechanical efficiency
$J$	Moment of inertia of the engine [ $Kg.m^2$ ]
$I_{tc}$	Moment of inertia of the turbocharger shaft [ $Kg.m^2$ ]
$H_f$	Fuel heating value [J/Kg]
$P_e$	Effective power produced by engine [W]
$P_r$	Friction power [W]
$C_r$	Friction torque [N.m]
$\lambda$	Air to fuel ratio
$D$	Diameter [m]
$M$	Mach number
$\pi_c$	Compressor compression ratio
$\pi_t$	Turbine relaxation ratio
$r$	Mass constant of air [J/(Kg. $^{\circ}K$ )]
$\gamma$	Ratio of heat capacities at constant pressure and volume
$C_p$	heat capacity at constant pressure [J/(Kg. $^{\circ}K$ )]
$C_v$	heat capacity at constant volume [J/(Kg. $^{\circ}K$ )]
BFGS	Broyden-Fletcher-Goldfarb-Shanno

SUBSCRIPTS	
$a$	Intake manifold
$e$	Exhaust manifold
$c$	compressor
$t$	Turbine
$f$	Fuel
$0$	Atmospheric conditions
$max$	Maximum value
$ref$	Reference value
$corr$	Corrected value

## CONTACT

[omranrabih@gmail.com](mailto:omranrabih@gmail.com)